Observation of a Nonmagnetic Hard Gap in Amorphous In/InO_x Films in the Hopping Regime

Ju-Jin Kim and Hu Jong Lee

Department of Physics, Pohang Institute of Science and Technology, Pohang P.O. Box 125, Kyungbuk 790-600, Korea and Division of Basic Science Research, Research Institute of Industrial Science and Technology, Pohang P.O. Box 135, Kyungbuk 790-600, Korea

(Received 2 December 1992)

We measured low temperature conduction characteristics of amorphous indium/indium-oxide composite films deep in the insulating regime. Upon lowering temperature, resistance crosses over from an Efros-Shklovskii variable-range-hopping conduction to a simple activation conduction, with parameters in good agreement with the picture of hardening of a parabolic Coulomb gap near the Fermi level. In contrast to the previous observations in magnetic materials, however, the hard gap in our films is extremely insensitive to a magnetic field, which strongly indicates a nonmagnetic nature of the hard gap.

PACS numbers: 72.20.Fr, 71.30.+h

The electron-electron interactions on the insulating side of the metal-insulator (MI) transition lead to a gap in the single-particle density of states (DOS) near the Fermi level [1-3]. Considering the single-electron hopping process, Efros and Shklovskii (ES) have shown that [3], in 3D, the mutual Coulomb interactions cause a smooth parabolic depletion of DOS of size Δ_C, centered at the Fermi energy E_F. Opening of this "soft gap," in turn, causes a deviation from Mott's variable-range-hopping (VRH) conduction of the form $\ln(\rho/\rho_0) \propto T^{-\nu}$ with $\nu = \frac{1}{4}$, which is obtained assuming a constant DOS [4]. The resulting ES variable-range hopping across the parabolic gap changes the value of the exponent ν into $\frac{1}{2}$. Such a Mott-to-ES crossover upon lowering temperature has been observed experimentally in several materials [5-7].

On the other hand, it has been pointed out that multiparticle excitations following a long-range electron hopping may be important at low temperatures [2,8-10], thereby giving rise to a DOS near E_F much sharper [5, 11] in variation than $|E-E_F|^2$. Subsequent work [12] has shown that stabilizing the ground state with respect to short-range polaron excitations near the initial and final sites of a long-range hopping causes a small but finite energy range near E_F with effectively vanishing DOS inside the parabolic Coulomb gap. The energy range, of order $\Delta_C/5$, is called a "hard gap." So electrons, transiting across the hard gap, may exhibit a conduction of simple thermal activation, $\ln(\rho/\rho_0) \propto T^{-1}$. The interactions between polarons can be either electric or magnetic, depending on whether the polarons possess electric dipole moments or magnetic moments. A crossover from the ES VRH to the hard-gap (HG) hopping (ES-to-HG crossover) with decreasing temperature has also been observed experimentally in several magnetic systems such as amorphous GeCr [13], ion-bombarded polyimide films [14], and ion-implanted Si:As samples [15]. Very recently similar behavior has been observed in other magnetic materials such as irradiated photoconductor $Cd_{0.91}Mn_{0.09}Te$:In [16] and uncompensated p-type Si:B [17]. The conduction characteristics in these materials were all interpreted in terms of the existence of a magnetic hard gap, arising from the interactions between localized magnetic moments. Since the hard-gap-hopping conduction, especially in the latter two materials, was very vulnerable to an external magnetic field the hard gap was claimed to be magnetic in origin.

In this paper we report the results of conduction measurements at low temperatures on homogeneous insulating amorphous indium/indium-oxide (In/InO_x) composite films, which we believe strongly indicate hardening of the parabolic Coulomb gap near E_F due to electrical polaron excitations. In clear contrast to the magnetic materials mentioned above, the conduction characteristics of our In/InO_x films in the hard-gap temperature regime were extremely insensitive to an external magnetic field. All the films retain the resistivity exponents ν intact up to 8 T all over the temperature range explored, this fact implying a nonmagnetic nature of the hard gap in these films. The small positive magnetoresistance [$\{R(H)-R(0)\}/R(0) \sim 0.1$ maximally, in $H=8$ T] observed in our films is also in clear contrast with the large negative magnetoresistance (MR) in the above-mentioned magnetic materials, except for Si:B which shows a large and positive MR [17]. The behavior of MR in our films can be described in terms of shrinkage of localized electron wave functions [18]. In zero field, the films show both the Mott-to-ES and the ES-to-HG crossovers. The Mott-to-ES crossover takes place at a temperature a little below the liquid nitrogen temperature, while the ES-to-HG crossover takes place at a temperature in the range 7-35 K, which corresponds to the size of the hard gap of an order $\Delta_C/2$. With increasing disorder, the crossover temperatures rise and the size of both the soft and the hard gaps widens.

In the regimes of Mott VRH and ES VRH, in 3D, zero-field resistance obeys exponential behavior, $R \propto \exp(T_M/T)^{1/4}$ and $R \propto \exp(T_E/T)^{1/2}$, respectively, with $k_B T_M = 18/N(E_F)\xi^3$ [4,18] and $k_B T_E \approx 2.8e^2/\varepsilon\xi$ [3,18], where $N(E_F)$ is the DOS at the Fermi level, ξ is the localization length, e is the electron charge, and ε is the dielectric constant of the films. For the Mott VRH [ES VRH], electrons hop over a range $R_M = \frac{3}{8}(T_M/T)^{1/4}\xi$ [$R_E = \frac{1}{4}(T_E/T)^{1/2}\xi$] between the initial and the final sites with an energy difference $\delta_M = \frac{1}{4} k_B T (T_M/T)^{1/4}$ $[\delta_E = \frac{1}{4} k_B T (T_E/T)^{1/2}]$. The size of the soft Coulomb gap is, then, given by [3,6]

$$\Delta_C \approx e^3 N(E_F)^{1/2}/\varepsilon^{3/2} = k_B (T_E^3/T_M)^{1/2}, \qquad (1)$$

which provides a way to estimate Δ_C from a measurement of T_M and T_E. We also estimate the Mott-to-ES crossover temperature to be $T_{ME} = 16(T_E^2/T_M)$, in 3D, by assuming that δ_M becomes comparable to δ_E at T_{ME} [6,19].

The homogeneous amorphous In/InO_x films were prepared by reactive ion beam sputtering of high-purity (99.999%) indium in an atmosphere of oxygen at pressure over the range of 6×10^{-5}–1.0×10^{-4} Torr. The films consist of small (~30 Å in diameter) amorphous indium grains embedded in an indium-oxide host. Since the average hopping length (~100 Å over the temperature range of the Mott VRH) in our films is larger than the grain size, the films can be considered homogeneous so that granularity effects can be ignored. Details of the characteristics of amorphous In/InO_x composite films prepared in this way are described in Ref. [20]. The thickness was kept fixed at 80 Å for all the films used. Various relevant parameters for the films are listed in Table I. Each film was patterned into a 4×1 mm^2 strip using a metal stencil. The distance between voltage lead contacts was 2.55 mm. Measurements were made using a standard four-probe technique in an Ohmic current regime over a temperature range of 0.5–160 K.

The inset to Fig. 1(a) shows the temperature dependence of zero-field resistance, over 0.5–100 K, of the five films S1–S5 with different sheet resistance at 4.2 K in the range 100 kΩ/□–1 GΩ/□. Resistance shows thermally activated behavior, following the general expression $\ln(\rho/\rho_0) \propto T^{-\nu}$ with $\frac{1}{4} \le \nu \le 1$. In Figs. 1(a) and 1(b) we plot $\log_{10}\{-d(\ln R)/d(\ln T)\}$ for the samples as a function of $\log_{10}(T)$ in a high and a low temperature region, respectively, where the slope of the fit lines corresponds to $-\nu$ [21]. Figure 1(a) clearly demonstrates that, for samples S3-S5 in the range 45–70 K, the value of the exponent ν changes from $\frac{1}{4}$ to $\frac{1}{2}$ as the temperature is lowered [22]. In Table I we list the best fit values for the characteristic temperature parameters T_M and T_E. The $T^{-1/2}$ dependence indicates that the conduction, below the crossover temperature T_{ME} for each film, is

TABLE I. Various characteristic sample parameters defined in the text. Some parameters for S1 and S2 are missing due to too high values of the Mott-to-ES crossover temperatures to be measured.

	R(4.2 K) (kΩ/□)	T_M (K)	T_E (K)	T_{ME} (K)	$T_{ME}^{\rm expt}$ (K)	Δ_C (K)	E_H (K)	Δ_H (K)
S1	1.04×10^6	···	394	···	···	···	30–40	~35
S2	4400	···	160	···	···	···	12–14	~14
S3	950	1631	84.0	69.2	77	19.1	10–12	~10
S4	230	665	46.9	52.9	56	12.5	7.0–7.5	~7.5
S5	132	372	33.3	47.7	48	9.97	~6.5	~7.0

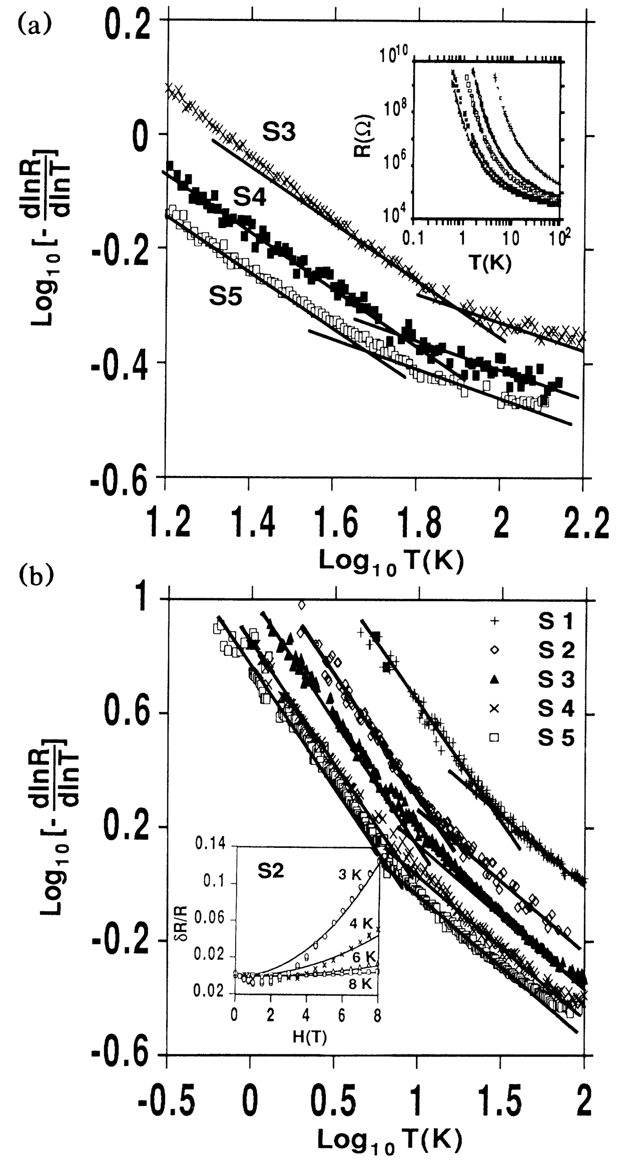

FIG. 1. Plots of $\log_{10}\{-d(\ln R)/d(\ln T)\}$ as a function of $\log_{10}(T)$. The slope of the fit lines correspond to $-\nu$. (a) The samples S3–S5 in the temperature range 15–160 K, showing the Mott-to-ES crossover. Inset: The temperature dependence of zero-field resistance of the five films S1–S5 sequentially from the top. (b) The samples S1–S5 in the range 0.5–100 K, showing the ES-to-HG crossover. The inset shows fitting of a fractional change in the MR for the sample S2 by Eq. (2) as a function of a magnetic field at temperatures 3, 4, 6, and 8 K.

governed by the ES VRH with electron-electron interactions. The values of $T_{ME} = 16(T_E^2/T_M)$ inferred from the predetermined parameters T_E and T_M are listed in Table I, together with $T_{ME}^{\rm expt}$ which is obtained by reading the cross point of the two best fit straight lines to the R vs T data in the region of Mott VRH and ES VRH. We see that the two values turn out to be very close to each other, confirming the self-consistency of the analysis employed. T_{ME} rises as the films become more resistive with increasing disorder.

The ES-to-HG crossover behavior in the samples S1-S5 is presented in Fig. 1(b) at lower temperatures in the range 7–35 K, where all the films show a clear change in the resistivity exponent from $\nu \approx \frac{1}{2}$ to $\nu \approx 0.85$–0.95, a value close to that of the simple thermal activation. The crossover behavior indicates that the ES VRH conduction is strongly modified due to hardening of the soft gap into the simple-thermal-activation conduction below a characteristic temperature $T_{EH} = \Delta_H/k_B$. The size of the Coulomb gap inferred from Eq. (1) with the values of T_M and T_E listed in Table I for the samples S3-S5 is in the range $\Delta_C/k_B \approx 2$–20 K, which is close to the ones observed by others in amorphous indium oxide and MoC films [5,6]. We see in the table that the ratio $k_B T_{ME}/\Delta_C$ for the samples S3-S5 turns out to be 3–5, which is in fair accord with the estimated value 2 [6,19]. Recently, a simple activation has also been observed by others in amorphous indium-oxide films [23], but only in the regime close to the MI transition and interpreted in a different context.

The existence of the hard gap can be confirmed further by examining the temperature dependence of the effective activation energy E_H obtained from the relation [24] $E_H(T) = d(\ln R)/d(1/T)$. The activation energies shown in Fig. 2 for the five films decrease continuously with decreasing temperature, which is one of the typical characteristics of a VRH, either Mott type or ES type. E_H for each film tends to converge to a constant value in the range 6.5–40 K in the low temperature limit, a demonstration of gradual hardening of the parabolic gap. The values of E_H are very close to Δ_H, which implies that the simple-activation behavior onsets with decreasing temperature as the thermal energy becomes comparable to the size of the hard gap E_H. E_H turns out to be of an order $\Delta_C/2$, which is a little larger than the theoretical estimate $\Delta_C/5$ inferred from polaron excitation model [12].

The inset to Fig. 3 shows R vs T for the samples S3 and S4 in a transverse external magnetic field of 8 T (open squares) together with the zero-field data (solid curves) for comparison. Both films are extremely insensitive to a magnetic field, showing only a small positive fractional change in resistance $\delta R/R \sim 0.1$ even in a field of 8 T. Both the sign and the magnitude of $\delta R/R$ are in clear contrast with the previous observations in the magnetic-hard-gap materials, where a change in magnitude by a factor of 2–10 is common in the similar field range in the low temperature limit used. We believe that a negative sign for MR as observed in most of the magnetic materials is more natural to the notion of destruction of a magnetic hard gap in high fields while the ES VRH is restored [16,17]. In this regard, the positive MR observed in the hard-gap temperature regime in our films can hardly be of a magnetic origin. We also notice in the inset that even the small deviation from the zero-field R vs T starts taking place only far below T_{EH}, which indicates that the MR in our films cannot arise from a magnetic-field modification of a hard gap. The insensitivity of $R(H,T)$ to a magnetic field is more clearly illustrated in Fig. 3, where again $\log_{10}\{-d(\ln R)/d(\ln T)\}$, both in zero field (solid curves) and in 8 T (symbols), is plotted as a function of $\log_{10}(T)$ for the two films. We see that the resistivity exponent is essentially unchanged with fields, and so is the nature of R vs T, all over the temperature range explored. A possible logical alternative for the mechanism of the hard gap in our films is, then, the multielectron interaction effect leading to electric polaron excitations, as first proposed by Chicon, Ortuno, and Pollak [12]. One may estimate the order of magnitude of an electric field E required to destroy the

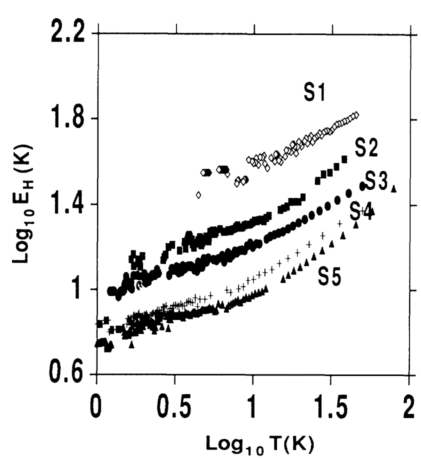

FIG. 2. The effective activation energy E_H obtained from the relation $E_H(T) = d(\ln R)/d(1/T)$ as a function of temperature.

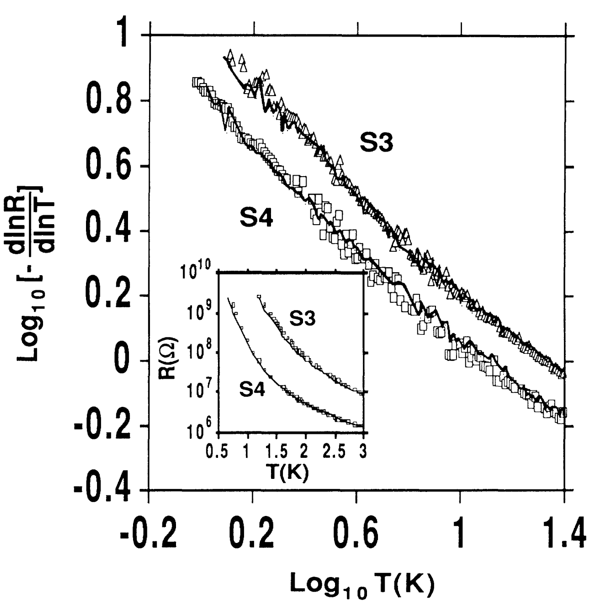

FIG. 3. A plot of $\log_{10}\{-d(\ln R)/d(\ln T)\}$, both in zero field (solid curves) and in 8 T (symbols), as a function of $\log_{10}(T)$ for the samples S3 and S4. Inset: R vs T in a linear plot for the samples.

electric hard gap by equating the dipole potential energy of a polaron in the field to the maximum interaction energy between dipoles a distance R_E apart. If we assume $P \sim e\xi$ as the maximum order of a polaron dipole moment we get, at $T=1$ K and for $\xi \sim 100$ Å, the magnitude of the required electric field $E \sim e\xi/R_E^3 \sim 10^8$ V/m, a value to which one may be marginally accessible experimentally. The MR of our films is also opposite both in magnitude and in sign to that of *granular* In/InO_x composite films [25]. The large (typically $\delta R/R \sim 0.9$ for 8 T at about 0.7 K) and negative MR observed in the granular films [25] was attributed to magnetic-field suppression of a superconducting gap present in the indium grains.

We found that the small positive MR of our films in the insulating regime, while in contradiction to the picture of field destruction of the hard gap, is well described by the model of shrinkage of the localized electron wave functions in an external magnetic field. According to the model, in a finite field at temperature T, the resistance is expected to follow the temperature and field dependence of the form [18]

$$\ln\left(\frac{R(H,T)}{R(0,T)}\right) \approx C\frac{\xi^4}{\lambda^4}\left(\frac{\Delta_H}{k_B T}\right)^{3\nu}, \qquad (2)$$

where C (≈ 0.0015) is a constant [18], $\lambda=(c\hbar/eH)^{1/2}$ is a characteristic magnetic length, and ν is the resistivity exponent defined as for the zero-field R vs T data above. Therefore, with $\nu \approx 1$ in Eq. (2) in the temperature range below T_{EH} we expect the temperature and field dependence of the resistance to be of the form $\ln[R(H,T)/R(0,T)] \sim \alpha T^3 H^2$, where $\alpha \approx C(e/c\hbar)^2(\Delta_H/k_B)^3\xi^4$ is a constant and H is in G. The inset to Fig. 1(b) shows the fractional change in the MR, $\delta R/R$, for the sample S2 below its T_{EH} in fields up to 8 T. The best fit by Eq. (2) is obtained with $\alpha = 4.19\times10^{-2}$–$4.97\times10^{-2}$ K^3T^{-2}, which corresponds to 81–85 Å for the localization length ξ. This value is quite close to the one observed previously in films of similar composition [6].

We believe that formation of the hard gap observed in various materials at a low temperature regime may have different mechanisms, either electric or magnetic, depending on the nature of a localized order a given material has. Experimental evidences collected to date appear to indicate that the magnetic correlation effects dominate the low temperature conduction properties in an insulating material with a localized magnetic order, while without the magnetic order, as in our films, the electric effects manifest themselves. More investigation is required to clarify the mechanism of formation and the nature of the hard gap.

We wish to thank M. Y. Choi and B. I. Min for useful discussions on the polaron excitations in disordered systems. This work was supported in part by Basic Science Research Center administrated by the Ministry of Education, Korea, under Contract No. N91126 and in part by Korea Science and Engineering Foundation, under Contract No. K92099.

[1] M. Pollak, Discuss. Faraday Soc. **50**, 13 (1970); G. Srinvivasan, Phys. Rev. B **4**, 2581 (1971).
[2] M. Pollak, Proc. R. Soc. London A **325**, 383 (1972).
[3] A. L. Efros and B. I. Shklovskii, J. Phys. C **8**, L49 (1975).
[4] N. F. Mott, J. Non-Cryst. Solids **1**, 1 (1968).
[5] Y. Zhang, P. Dai, M. Levy, and M. P. Sarachik, Phys. Rev. Lett. **64**, 2687 (1990), and the references cited therein.
[6] R. Rosenbaum, Phys. Rev. B **44**, 3599 (1991).
[7] S. J. Lee, J. B. Ketterson, and N. Trivedi (to be published).
[8] A. L. Efros, J. Phys. C **9**, 2021 (1976).
[9] N. F. Mott, J. Phys. C **8**, L239 (1975).
[10] M. Mochena and M. Pollak, Phys. Rev. Lett. **67**, 109 (1991).
[11] J. H. Davies, P. A. Lee, and T. M. Lee, Phys. Rev. Lett. **49**, 758 (1982).
[12] R. Chicon, M. Ortuno, and M. Pollak, Phys. Rev. B **37**, 10520 (1988).
[13] A. N. Aleshin *et al.*, Fiz. Tverd Tela (Leningrad) **30**, 696 (1988) [Sov. Phys. Solid State **30**, 398 (1988)].
[14] A. N. Aleshin, A. V. Suvorov, and I. S. Shlimak, Solid State Commun. **71**, 85 (1989).
[15] R. W. van der Heijden *et al.* Solid State Commun. **78**, 5 (1991).
[16] I. Terry, T. Penney, S. von Molnar, and P. Becla, Phys. Rev. Lett. **69**, 1800 (1992).
[17] P. Dai, Y. Zhang, and M. P. Sarachik, Phys. Rev. Lett. **69**, 1804 (1992).
[18] B. I. Shklovskii and A. L. Efros, in *Electronic Properties of Doped Semiconductors,* edited by Manuel Cardona, Solid State Science Vol. 45 (Springer-Verlag, Berlin, 1984).
[19] T. G. Castner, in *Hopping Transport in Solids,* edited by M. Pollak and B. I. Shklovskii (Elsevier/North Holland, Amsterdam, 1990), p. 1.
[20] A. F. Hebard and S. Nakahara, Appl. Phys. Lett. **41**, 1130 (1982).
[21] A. G. Zabrodskii and K. N. Zino'eva, Zh. Eksp. Teor. Fiz. **86**, 727 (1984) [Sov. Phys. JETP **59**, 425 (1984)].
[22] The conductivity exponent indicates that the films are in the 3D limit, although the hopping length estimated from the localization length ξ, which was obtained in turn from a best fit to the MR as in the inset of Fig. 1(b), should put the samples in the 2D limit. We suppose that the apparent contradiction originated from the uncertainty which may have been present in estimating ξ. In fact, the relative magnitude of the hopping length to the film thickness is marginal, so that a sample (not quoted in the text) with the sheet resistance with 44 kΩ/□ at 4.2 K shows a better fit to the $\frac{1}{3}$-power conductivity in the Mott VRH regime.
[23] D. Shahar and Z. Ovadyahu, Phys. Rev. B **46**, 10917 (1992).
[24] Although multielectron excitations are important in stabilizing the ground state as stated in the text the one-electron excitation picture is adopted in the analysis of this simple activation.
[25] J. J. Kim, J. Kim, and H. J. Lee, Phys. Rev. B **46**, 11709 (1992).